ELSEVIER

Bioelectrochemistry and Bioenergetics 45 (1998) 73–81

BIOELECTROCHEMISTRY AND BIOENERGETICS

Interference mechanism for some biological effects of pulsed magnetic fields

V.N. Binhi *

International Institute of Theoretical and Applied Physics RANS, P.O. Box 214, Moscow 125190, Russian Federation

Received 16 May 1997; revised 26 December 1997; accepted 9 January 1998

Abstract

A mechanism that describes effects of a pulsed magnetic field (PMF) of ELF range on some biological systems is presented. This mechanism, based on earlier proposed ion interference mechanism, links the dissociation probability of ion-protein complexes to parameters of PMF. Quantum dynamics of ion is studied in the case of PMF combined in line with a static magnetic field. A rule that enables us to reach a maximal biological response on PMF is found. The formula is derived for the first time for biological efficacy of a PMF. Calculations were made for Ca- and Mg-protein complexes. The results show a good consistency with known experimental data.

Keywords: ELF PMF; Ion binding; Quantum dynamics; Interference; Calcium

1. Introduction

There is much evidence that weak ELF magnetic fields (MFs) can affect living matter: cells, tissues, and hole organisms. In many cases, these effects resemble a resonance. The frequency and amplitude dependences of relevant biological endpoints demonstrate a complex polyextreme spectral form. Numerous attempts were undertaken to explain a physical origin of the phenomenon on the basis of known physical resonant processes. The cyclotron resonance in biology [1] and other oscillatory mechanisms were reviewed, for example, in Refs. [2–4]. The general conclusion derived from fitting the models to experiments is that one of the most likely targets for MF in living matter is a process of ion binding with proteins.

In Ref. [5], a quantum mechanics was used to describe ion states within a binding cavity of the protein. An idealized case was studied of the ion placed in a central potential and exposed to the MF modulated in its magnitude. The value of MF-induced biological effect was assumed to depend on the probability of ionic quantum transitions. However, this idea is weakly consistent with that of the above MF, affecting only the phases of quantum states does not actually cause the transitions. The population of each quantum state is exactly constant regardless of the MF parameters. The same inference is valid for the models based on the analogy with so-called parametric resonance in atomic spectroscopy. Another idea [5] was that biological effects of MFs depend on the probability of ion to be inside a small virtual sphere centered within the cavity; no final formula has been derived for that probability.

There are a lot of other models where bioeffects are associated with resonant quantum transitions in Zeeman sublevels. The analysis is obstructed because of the failure of those models to obtain mathematical formulas for effective magnetic parameters and to formulate predictions for experimental tests.

Recently, a mechanism was suggested [6,7] that develops quantum-mechanical approach [5] and can predict effective parameters of weak magnetic fields. The mechanism is based on an interference of quantum states of ions bound to protein inside an idealized cavity. Superposition of ion states forms an interference pattern of the probability density of ion. This pattern consists of a row of more and less dense segments. In static MF, the pattern rotates as whole with the cyclotron frequency. Exposure to ac MFs can retard the rotation during a large part of the rotation period. It facilitates the escape of ion from the cavity and shifts a biochemical balance.

* Corresponding author. 21/7, B. Dmitrovka St., Kv.31, Moscow 103009, Russian Federation. Tel.: +7-095-292-9589; fax: +7-095-292-9589; e-mail: binhi@dataforce.net

The predictions of the ion interference mechanism appeared to be in a good agreement with some effects of collinear static and ac MFs. The mechanism also accounts for the biological effects of the MFs with the frequency of a proton magnetic spin resonance [7,8]. It follows that interference of quantum ion states is likely to be a physical basis for some magnetobiological effects of collinear static and sinusoidal MFs. At the same time, many experiments were made with biological systems exposed to PMFs; there is much biomedical application of such fields [9,10]. In present work, the extension is presented of the ion interference mechanism to the case of PMFs, theoretical predictions is compared with known experimental results.

2. Sinusoidal MF

The ions inside the protein cavities will be regarded as described previously in Ref. [6]. The Hamiltonian operator of the Schroedinger equation for an ion with charge q and mass M (without spin) exposed to an MF H in a central potential U is as follows [11]:

$$\mathscr{H} = \frac{P^2}{2M} + U - \frac{q\hbar}{2Mc} L\boldsymbol{H}.$$

Here $P = -i\hbar\nabla$ is the momentum operator and $L = -ir \times \nabla$ is the angular momentum operator. The ion enter to or escape from the cavity at a point which is called ionic gate. The notion of ionic gate is a general mathematical idealization rather than geometry of the cavity. The gate is a sight where ion could escape the cavity due to a quantum tunnelling. For example, Ca-binding cavity in the troponin-C protein has an octahedral arrangement of the binding ligands forming the cavity. Therefore, there are several places between the ligands, where the tunnelling of bound ion is easier. The probability of such a tunnelling in a finite time interval obeys the Poisson flow statistics. The MF can affect this process resulting in a biological effect. Given the MF $H_{\rm dc} + h(t)$ in parallel with z-axis, the probability density of ion near the ionic gate with angular position $\varphi = \varphi_0$ is:

$$p(\varphi_0, t) = \sum_{mm'} a_{mm'} \exp\left[i\Delta m \left(\varphi_0 + \omega_0 t + b \int_0^t h(t)\, dt \right) \right], \quad (1)$$

where $b = q/2Mc$, $\omega_0 = b\, H_{\rm dc}$, $\Delta m = m' - m$, $m = 0, \pm 1, \ldots$ is the magnetic quantum number. The matrix elements $a_{mm'}$ are constants, which determine the initial conditions of ion entering cavity at $t = 0$. For example, a_{mm} is an initial population of the state with magnetic quantum number m.

In general, the probability of escape P depends nonlinearly on the ionic density (Eq. (1)) near the gate. The dependence may be written as a polynomial series near the permanent component $\bar{p}$ of p. Two initial terms, linear and quadratic, of the expansion $P(p) = P(\bar{p}) + P'_p \tilde{p} + \frac{1}{2} P''_{pp} \tilde{p}^2 + \ldots$, where $\tilde{p} = p - \bar{p}$, are left for analysis. Averaging over the time, we get $\bar{P} = c_1 + c_2 \overline{\tilde{p}^2}$, where $c_{1,2}$ are constant values. The expression for mean probability of dissociation has several components. The part $P = \overline{\tilde{p}^2}$ presents a dependence of $\bar{P}$ on the MF parameters and will be analyzed. In order to simplify calculations, relatively fast oscillations of p are neglected. For this purpose, the average of $\tilde{p}$ over the mean time T of conformational reaction of the protein was found beforehand, that is, $T[\tilde{p}]$. The value T may be thought as the characteristic time for the dissociation of ion-protein complex. This time was found about 0.05–0.1 s in Ref. [12] for binding of calcium to calmodulin. The final expression for mean 'magnetic' component is $P = \overline{T[\tilde{p}] \cdot T[\tilde{p}]}$. If $h(t) = H_{\rm ac} \cos(\Omega t)$ the P is as follows [6]:

$$P = \sum_{mm'n} |a_{mm'}|^2 \frac{\sin^2 A}{A^2} J_n^2 \left(\frac{\Delta m}{2} \frac{h'}{f'} \right),$$
$$A = \left[\Delta m \frac{1}{2} + nf' \right] \Xi, \quad (2)$$

where $f' = \Omega/\Omega_c$ and $h' = H_{\rm ac}/H_{\rm dc}$ are dimensionless frequency and dimensionless peak value of MF, $\Omega_c = qH_{\rm dc}/Mc$ is the cyclotron frequency. J_n is the nth order Bessel function of the first kind, $\Xi = T\Omega_c$ is the dimensionless product, which controls a width of peaks of P: $\Delta f' \approx \pi/\Xi$.

It has been shown in Ref. [7] that the formula (2) fits some experimental spectra of MF action on *Escherichia coli* [13], land snail, and planarian organisms. The range of populated angular modes in all the cases was the same: $m = -2,..,2$, m' runs the same set of values. Allowance for higher modes altered slightly only the form of peaks. The value of Eq. (2) as a row over n converges quickly so that $n = -3,..,3$ provides good approximation to Eq. (2). Results of comparison with other experiments [1,14,15] which were performed in a collinear dc and sinusoidal MF,

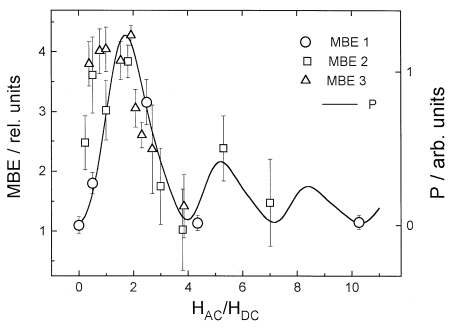

Fig. 1. Comparison between the theoretical amplitude spectrum of the ion interference (P) and experiments: data [1] on the calcium uptake in human lymphocytes (MBE 1), data [14] on the latency of avoidance response of land snail (MBE 2), data [15] on the fibroblast cell proliferation (MBE 3).

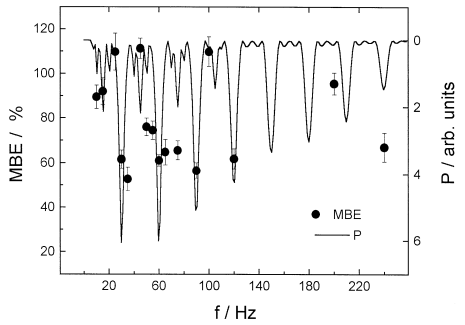

Fig. 2. Experimental frequency spectrum [14] measured with collinear $B_{dc} = 78.1$ μT, $B_{ac} = 141$ μT (MBE), and the curve calculated for ^{40}Ca with formula (2) at the same magnetic conditions (P).

are displayed here to emphasize the reality of the ion interference.

Calcium ^{45}Ca uptake in human lymphocytes exposed to variable MF was investigated in Ref. [1]. The experimental design was chosen to meet the conditions for ^{45}Ca cyclotron resonance: $B_{dc} = 21$ μT, $f = 14.3$ Hz, $B_{ac} = 0$–220 μT. Theoretical amplitude spectrum was calculated using Eq. (2) at the cyclotron frequency, that is, $f' = 1$, in the range of relative amplitude $h' = 0$–11 with the above mentioned values for numbers m and n. All elements $a_{mm'}$ were equal to unit. The calculated curve was then superposed on the experimental points of the magnetobiological effect (MBE) and scaled vertically to best fit. Data of Ref. [14] obtained at $B_{dc} = 78.1$ μT, $f = 60$ Hz, $B_{ac} = 20$–550 μT for the latency of avoidance response of land snail on a thermal stimulus, in relation to sham-exposure, are superposed on the above data as well. In addition, the data were processed in the same way, on the fibroblast cell proliferation at $B_{dc} = 130$ μT, $f = 100$ Hz tuned for ^{40}Ca-ion, $B_{ac} = 50$–500 μT [15]. Fig. 1 shows the results. It is seen that the theory does not contradict the experiments.

A frequency spectrum of magnetobiological effect in a land snail has been studied in Ref. [14] at parallel $B_{dc} = 78.1$ μT, $B_{ac} = 141$ μT also. The spectrum was of a polyextreme shape and so suited for comparison with the theory. The computation was performed with formula (2), for Ca ion at the same magnetic conditions, that is, $h' = 1.8$. Other parameters were $m = -4,..,4$, for the spectral details to be seen, $n = -3,..,3$, $\Xi = 27$, $a = 1$. Both the experimental points and computed curve are shown in Fig. 2. They do not contradict each other. At the same time, quantity of points is not enough to identify spectral peaks in a reliable way.

3. PMF

The increase of ion escape probability, as was shown in Ref. [6], is accounted for by a 'freezing' of the phase difference of interfering angular modes $\exp(im\varphi)$ of the ion wave function. That means the phase difference is to be approximately constant during a large part of its period. That is, for the sequence of MF pulses to be effective, the change of phase difference in the time t due to the term $\omega_0 t$ in Eq. (1) must be compensated by phase changes due to the MF pulses $h(t)$.

Let the PMF be written as a sequence of δ-pulses of intensity ξ, coming at frequency f:

$$h(t) = \xi \sum_{k=-\infty}^{\infty} \delta(t - f^{-1}k).$$

The sequence approximates, for example, rectangular pulses of magnitude h and duration τ at $\tau h = \xi$, separated by periods f^{-1}.

The change of the phase difference due to the static field $\Delta m \omega_0 t$ will be compensated, if the MF pulses alter the phase difference by $2\pi r - \Delta m \omega_0 t$, $r = 0, \pm 1,..$ at the same time. One pulse appears in the time f^{-1}. Phase increment is $\Delta mb\xi$, as follows from Eq. (1). Equating these values, we obtain the relation, $\Delta mb\xi = 2\pi r - \Delta m \omega_0 f^{-1}$, which defines magnetic conditions for maximums of P:

$$h\tau = \frac{1}{b}\frac{2\pi r}{\Delta m} - \frac{H_{dc}}{f}. \qquad (3)$$

It links the pulse intensity $h\tau$ with the value of static MF and parameters of ion, through the coefficient $b = q/2Mc$.

Detailed derivation (see Appendix A) results in the next formula for the dissociation probability of an ion-protein complex in a PMF along with a static MF. In designations $x = \Delta m \omega_0 / f$, $y = \Delta mb\xi$ the formula is as:

$$P = \sum_{mm'r} |a_{mm'}|^2 \left(\frac{\sin(x/2)}{x/2}\right)^2 \times \left(\frac{\sin[(x + y + 2\pi r)Tf]}{[(x + y + 2\pi r)Tf]}\right)^2. \qquad (4)$$

The ranges of PMF parameters define limits of summation on r. It follows from the formula that the relation $x + y + 2\pi r = 0$ must be satisfied for maximal value of P. This leads exactly to rule (3).

The same pulse intensity $\xi = h\tau$ may be obtained in different manners. However, unlike wide and low pulses, narrow and high pulses of the same product $h\tau$ induce appreciable eddy electric currents. This can cause biological effects of other physical nature, thermal or galvanic.

There is a frequent explanation of PMFs bioeffects, which relates to electric currents induced by PMFs in biological tissue [16,17]. This mechanism predicts that bioeffects, in some range, vary directly as the induced currents, in proportion to the time-derivative of the MF. At

least, there must be a correlation between the level of induced electric field and bioeffects. Such a correlation was observed, for example, in Ref. [18], where a cell proliferation has been investigated in a sinusoidal 2.8-mT 50-Hz MF. Cell (human HL-60) growth was affected by the uniform MF only where the induced electric field exceeded a threshold of 4–8 mV/m. At the same time, there is much experiment showing a failure of this prediction in the case of relatively weak ELF ac MFs [1,15,19–22]. For example, in Ref. [15], there were used different MFs satisfying the certain 'cyclotron' condition $\pi f/b = H_{dc} = H_{ac}$ tuned for Ca-ion. The product fH_{ac}, that is, the level of induced electric field, varied 40-fold throughout the MFs used, however, the significant biological effect of these MFs was invariant. This indicates that there might be other mechanisms underlying biological effects of weak PMFs.

This paper is aimed at explanation of bioeffects of relatively small PMFs, which cannot induce electric field strong enough for galvanic or thermal phenomena in biological tissue. Therefore, we find the PMF range suitable for the mechanism discussed.

The limit values are fixed by various standards for the safe levels of ELF MF exposure. The limits of exposure in public areas set by CENELEC 50166-1 is reduced to the definite rule. According to it, the frequency f in the range 1–1000 Hz and the amplitude h of the sinusoidal MF are to satisfy the relation:

$$hf < k_C = 3 \times 10^4\ \mu\mathrm{T/s}. \qquad (5)$$

This value has only a conditional physical meaning because the induced electric fields depend on the specific design of the MF sources. The level (Eq. (5)) may be understood as a well-averaged value. It is agreed that lower expositions cannot cause ordinary galvanic or thermal bioeffects. Nevertheless, such exposures can cause biological effects similar to a resonance [1,3,13,14]. Therefore, we use this limit with respect to the ion interference mechanism to define conditions of the interference manifestations.

Along with other physical constraints (see Appendix B) the limit leads to the inequalities that define values of the static MFs, in which one might observe complex (of two peaks) spectra of bioeffects in PMFs:

$$\frac{\pi}{2bT} < H_{dc} < \sqrt{\frac{\pi^2 k_C}{32\,b}}\ . \qquad (6)$$

This inequality means that not all ions, which are specified by a charge-to-mass ratio $b = q/2Mc$, are suitable to display polyextreme spectra in PMFs. Fig. 3 depicts b-dependences of the left and right quantities in Eq. (6) confining the value of the static MF. Values of b for different

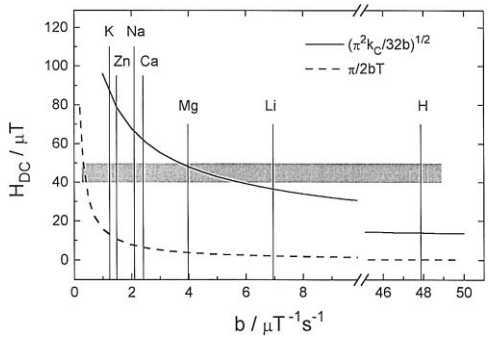

Fig. 3. Upper and lower limits confining the value of the static MF (Eq. (6)) suitable for measuring polyextreme spectra of the ion interference in PMF, from the charge-to-mass ratio b of an ion.

ions are indicated. As is seen, in static MFs of the geomagnetic level of middle latitudes, 40–50 μT, ions K, Na, Ca, Mg, Zn suit the mechanism discussed, and light ions of Li and H appear to be out of the band and require lower static MFs. The interference mechanism might be observed even at larger values of static MF than the upper limit (Eq. (6)), but for the increasing probability of the effects of other physical nature. Optimal PMF parameters for the ion interference with suitable values of static MF are given in Appendix B.

Rule (3) cannot be satisfied in true way if the product of pulse intensity $h\tau$ and pulse frequency f is less than the static MF H_{dc}. The mechanism is unable to account for the biological effects of PMF in this case. Such effects of very weak PMFs are known [23,24], $h\tau f \approx 0.05$ μT in both studies, though the level of their reproducibility leaves something to be desired.

In Ref. [25], the PMF-induced redistribution of transmembrane proteins at a cell surface was investigated in static MF 196 μT. The significant effect was reported with triangular pulses at 50 Hz, so that $h\tau f \sim 850$ μT. This relatively large value compared to the static field, the pulse shape far from the δ-form, and proximity of its fundamental harmonic to the standard ELF MF galvanic/thermal limit (Eq. (5)) make the interference mechanism hardly applied to this case. At the same time, there are no evident contradictions.

Some parameters of RNA synthesis in salivary gland cells exceeded the control values 11- to 13-fold after the exposure to ELF (15 and 72 Hz) PMFs [16]. A great difference was seen between biological effects of these PMFs, but neither sufficient description of the pulses nor the local static MF was reported. PMFs of 75 Hz induced a 2- to 5-fold increase of DNA synthesis in human osteoblast-like cells [26]; the assessment is feasible based on the incomplete PMF description, $h\tau < k_C$. That is, the PMF fell into the range covered by the interference mechanism. RNA and mRNA synthesis increased 2- to 3-fold, relative to control, in cells from the T-limphoblastoid cell line, which have been exposed to a quasi-rectangular 72

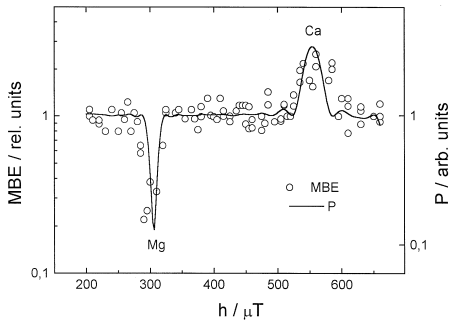

Fig. 4. Dissociation probability of Ca- and Mg-protein complexes under the PMF vs. the pulse magnitude h, computed with formula (4) at $f = 50$ Hz, $\tau = 13$ ms, $H_{dc} = 50$ μT (P); experimental data [28] on the relative rate of β-galactosidase synthesis (MBE).

Hz PMF [27]. The MF description was also insufficient to make the theoretical analysis.

A comparison between the theory and known experiments is impeded because of incomplete data about MF used in the experiments. For example, only a third of 27 reports [9], which were devoted to biological and biomedical applications of PMFs, have described PMF accurately. There were no reports utilizing PMF with a finely variable parameter. Of all the reports, no one indicated the value of a local static MF.

Influence of a PMF on inducible lac operon in *E. coli* was investigated in Ref. [28]. The rate of transcription of the β-galactosidase gene was measured. It appeared that a PMF could alter the rate. The cells were exposed to the PMF of a square waveform at 50 Hz during 2 h. There was an observed polyextreme dependence of the rate of the synthesis on the pulse amplitude in the range 200–660 μT. The rate was less than the control level by a factor of 4 at 300 μT and more than that by a factor of 2.5 at 550 μT, Fig. 4. The primary target for the PMF was assumed to be in a repressor protein, which can suppress the transcription.

Forcing the formula (Eq. (4)) to fit the experiment was as follows. The experiment shows two peaks of the effect in opposite directions. Therefore, two different ionic species, calcium ^{40}Ca and magnesium ^{24}Mg, were supposed to form the opposite peaks, since these ions can compete for binding sites. For both the species, the same range of the quantities $m = -1,\ldots,1$, $r = -2,\ldots,2$ were used. The PMF was similar to the experimental one: $f = 50$ Hz, $h = 200$–660 μT. The authors of Ref. [28] have not pointed out the value of the local static MF. Therefore, static MF of order of the geomagnetic one $H_{dc} = 50$ μT was used. The pulse duration and the reaction time were found $\tau = 0.013$ s and $T = 0.2$ s, correspondingly. With these values, the calculated positions of extrema and their width fitted the experimental peaks in the best way. The pulse duration $\tau = 0.013$ s and that used in Ref. [28] (a square wave PMF) were about of the same order. At last, the relative weights of contributions of Ca and Mg ions were 1.3 and -0.5, respectively, to provide a good coincidence in magnitudes of the peaks. Fig. 4 displays the result of superposition of the calculated curve and experimental points. As is seen, they are in a good agreement. We could not pick up another pair of ion species with the same result.

The 14%, $P = 0.03$, increase in the negative surface charge of human U937 cells exposed to a PMF has been reported in Ref. [29]. The PMF of $f = 25$ Hz frequency was comprised of $N = 22$ pulse bursts of a triangular shape, with the $\tau_1 = 200$ μs rise and the $\tau_2 = 20$ μs fall. The magnitude of pulses was $h = 630$ μT. At this case, the entire burst may be considered as a single pulse, as far as the burst duration is less than the time interval between bursts. The intensity of the composite pulse equals $\xi = Nh(\tau_1 + \tau_2)1/2$. The value of a static MF was not reported. Therefore, the agreement between the mechanism discussed and this experiment may be in that the calculated value for H_{dc} after rule (3) does not contradict the value of the local static field. The last is usually less than 50 μT in absolute value.

For example, the zeroth maximum of the P $(r = 0)$ with the PMF like in Ref. [29] is calculated at $H_{dc} = -38.1$ μT. Note that rule (3) at $r = 0$ means the mutual compensation of the local dc field and a constant constituent of the PMF. Consequently, the calculated peak does not depend on ion species. At $r = 1$, $\Delta m = 1$, we find $H_{dc} = 36.7$ μT for Na ions, $H_{dc} = 27.1$ μT for Ca ions. The computed values of H_{dc} for Mg, K, Zn are less than 50 μT and plausible as well. It follows that predictions of the ion interference mechanism in PMF do not contradict the observations [29].

4. Discussion

Usually, ions are regarded as classical particles. However, at the atomic scale, ions display quantum properties that cannot be reduced to some particular classical behavior. For the most ions of biological relevance, the de-Broglie wavelengths at 300 K are three to four times less than their ionic radii, that is, of the same order that the binding cavity size. Therefore, a quantum mechanics appears to be necessary to describe ion states within the cavity. An interference wave phenomenon, which underlies the ion interference mechanism, disappears in a classical limit, when an ion is a particle and not a wave. Consequently, a consistency between the interference mechanism and polyextreme magnetobiological spectra, which are experimentally observed, means a failure of a classical mechanics to explain such ELF MF bioeffects [30]. However, at larger scales, classical treatment may be applied to ions with a very good accuracy.

Another idealization is a one-particle approximation with regard to an ion, many-particle atomic system. This is

based on the known adiabatic approach, which is applicable when the system includes both slow and fast variables. Then the slow motion may be described 'adiabatically', that is, in time-averaged effective field that fast variables create. In our case, slow and fast dynamics relate to ionic nucleus and electrons, respectively. The electrons provide an ion with a quasielastic envelope that moves slowly with the nucleus and determines an ionic radius. Known experiments on the interference of atoms in atomic beams demonstrate the possibility of neglecting nonvalent electrons in relevant cases.

The effect described by formulas (2) and (4) is based on an interference phenomenon and, in general, has nothing to do with a resonance. It is a resonance-like ion interference. The uniaxial MF used in the interference mechanism affects only phases of angular modes. Therefore, the energy required for the ion interference is extremely small. It may be estimated as $< \hbar \Omega_c$. The mechanism explains why as small as ELF MF stimuli cause effects of the kT-comparable level. The stability of the angular modes may be illustrated in a simplified manner as follows. Thermal disturbances of the cavity walls do not agitate transitions between angular modes $\exp(im\varphi)$ of different m, the Zeeman sublevels, unlike modes of radial and azimuth quantum numbers. The energy or frequency scale of thermal oscillations is 10 orders higher than that of the Zeeman splitting. Thermal disturbances in an ELF range have a large wavelength, > 10 m, and cannot find enough room in biological systems. Therefore, the probability of thermally induced quantum transitions in the Zeeman states is a relatively small value of the second order of the perturbation theory. This means that the fairly large lifetime of the angular states: a projection of the angular momentum on the MF direction is conserved over a long period of time. This time was assumed here to be of order of or greater than the conformational reaction time $T \sim 0.1$ s. Quantitatively, the question of why the kT-level thermal disturbances do not destroy the interference or, in other words, why there is a thermal stability of the interfering angular modes, is a subject of a separate study. It is based on a nonlinear quantum dynamics and will be submitted elsewhere.

The formula for frequency spectrum in sinusoidal MF (along with a static field) [6,7] predicts a monotonous series of the effective frequencies: Ω_c, its harmonics and subharmonics. Unlike this, relation (4) predicts values that one could not refer to as a priori evident frequencies. Therefore, rule (3) provides a simple way of its own verification. Biological effect does not alter within some narrow limits when the magnitude and pulse duration of PMF vary so that their product remains constant. The same is to be true when the PMF frequency varies directly as the static MF. It should be emphasized that rule (3) is strongly associated with the mechanism of ion escape based on the interference of ion quantum states. For this reason, unambiguous conclusions are possible about the physical nature of magnetobiological effects in the case the rule is valid. A qualitative prediction follows the mechanism as well. Biological effects in a parallel pulsed and static MFs should be observed for those ionic species that display such effects in a parallel sinusoidal and static MFs or in a magnetic vacuum.

Acknowledgements

The author thanks Prof. A.E. Akimov and Prof. I.Ya. Belyaev for valuable comments and Prof. Yu.A. Chizmadzhev for stimulating discussion.

Appendix A

Find the integral over time from the sequence of MF δ-pulses:

$$\int_0^t \xi \sum_{k=-\infty}^{\infty} \delta(t - f^{-1}k)\mathrm{d}t = \xi \sum_k \Theta(ft - k),$$

where Θ is a unit function $\Theta(x) = 0,\ x \le 0, = 1,\ x > 0$. Substitution in $p(\varphi_0, t)$, Eq. (1) leads to:

$$p(\varphi_0, t) = \sum_{mm'} a_{mm'} \times \exp\left[i\Delta m\left(\varphi_0 + \omega_0 t + b\xi \sum_k \Theta(ft - k) \right) \right].$$

Consider the mean value over time interval $2T = (t, t + nf^{-1})$:

$$T[p] = \frac{1}{nf^{-1}} \int_t^{t+nf^{-1}} p(\varphi_0, t')\mathrm{d}t' = \frac{1}{n} \sum_{mm'} a_{mm'} \times \exp(i\Delta m\varphi_0) \otimes \int_\tau^{\tau+n} \times \exp\left[ix\tau' + iy \sum_k \Theta(\tau' - k) \right] \mathrm{d}\tau', \quad (7)$$

where:

$$x = \Delta m \frac{\omega_0}{f},\ y = \Delta m\, b\xi,\ \tau = ft.$$

Let an auxiliary variable t be defined as $t = \tau' - \tau$, then the integral in Eq. (7) may be written in the form:

$$I = \exp(ix\tau)\ I',\ I' = \int_0^n \exp\left[ixt + iy \sum_k \Theta(t + \tau - k) \right] \mathrm{d}t.$$

Note that:

$$\sum_k \Theta(t + \tau - k) = 1 + \sum_k \Theta(t + (\tau - 1) - k),$$

that is, the shifts of a right-up endless unit ladder leftward and upward are equivalent. We obtain:

$$\sum_k \Theta(t+\tau-k) = \tau + \sum_k \Theta(t-k).$$

Then:

$$I' = \exp(iy\tau)\, I'',\ I'' = \int_0^n \exp\left[ixt + iy\sum_k \Theta(t-k)\right]\mathrm{d}t.$$

Similarly:

$$\sum_k \Theta(t-k)_{|t\in(-1,0)} = \sum_k \Theta(t-k)_{|t\in(0,1)} - 1.$$

Let the left part of the last equality be denoted as ζ. Conversions of the integral I'' result in:

$$\begin{aligned} I'' &= \int_0^1 \exp(ixt)\exp[iy(\zeta+1)]\mathrm{d}t \\ &\quad + \int_1^2 \exp(ixt)\exp[iy(\zeta+2)]\mathrm{d}t + \ldots \\ &\quad + \textstyle\int_{n-1}^n \exp(ixt)\exp[iy(\zeta+n)]\mathrm{d}t \\ &= \exp(iy\zeta)\sum_{l=1}^n \exp(iyl)\textstyle\int_{l-1}^l \exp(ixt)\mathrm{d}t. \end{aligned} \quad (8)$$

The last integral equals:

$$\textstyle\int_{l-1}^l \exp(ixt)\mathrm{d}t = \frac{2}{x}\exp[ix(l-1/2)]\sin(x/2).$$

Then, substituting back to I'', I', I, we have:

$$I = \exp\left[i(x+y)\tau + iy\zeta - i\frac{x}{2}\right]\frac{\sin(x/2)}{x/2}S,$$

$$S = \sum_{l=1}^n \exp[i(x+y)l]. \quad (9)$$

Substituting Eq. (9) to Eq. (7) gives:

$$\begin{aligned} T[p] &= \frac{1}{n}\sum_{mm'} a_{mm'}\exp \\ &\quad \times\left[i\Delta m\varphi_0 + i(x+y)\tau + iy\zeta - i\frac{x}{2}\right]\frac{\sin(x/2)}{x/2}S. \end{aligned}$$

Calculating $P = \overline{T[p]\cdot T[p]}$, we note that only complex conjugate terms of $T[p]$ make contribution, which does not disappear after final averaging over time. Taking into account proportionality $x \propto \Delta m$, $y \propto \Delta m$, we may write:

$$P = \frac{1}{n^2}\sum_{mm'} |a_{mm'}|^2 \left(\frac{\sin(x/2)}{x/2}\right)^2 S * S.$$

Maxima of P are at x, y such that value of $S * S$ equals its maximal quantity, that is, at $x + y = 2\pi r$, $r = 0, \pm 1, \ldots$ Substitution of designations for x, y results exactly in rule (3) of maximums of P in pulsed MF. At $r = 0$, the rule is rewritten as $\xi f = -H_{dc}$ that means the constant constituent of MF pulses compensates the static MF.

To assess $S * S$, summation over l should be changed by integrating:

$$S = \sum_{l=1}^n \exp[i(x+y)l] \to \int_0^{2Tf} \exp[i(x+y)v]\mathrm{d}v.$$

However, the important property is lost $S(x+y) = S(x+y+2\pi r)$, $r = 0, \pm 1, \ldots$ To save it, we write S in equivalent form:

$$S = \sum_{l=1}^n \exp[i(x+y+2\pi r)l].$$

Now, coming to integration, we obtain the assessment of $S * S$:

$$\begin{aligned} &\sum_{r=-\infty}^{\infty}\left|\int_0^{2Tf}\exp[i(x+y+2\pi r)v]\mathrm{d}v\right|^2 \\ &\quad = 4\sum_r \frac{\sin^2[(x+y+2\pi r)Tf]}{(x+y+2\pi r)^2}. \end{aligned}$$

Substituting this in the last relation for $\mathscr{P}$ we have the result (Eq. (4)).

Appendix B

As follows from the multiplier $\sin(x/2)/(x/2)$ in Eq. (4), the value of $x = \omega_0 f^{-1}\Delta m$ should be sufficiently small. It means that the angular shift of the ionic interference pattern in the time f^{-1} must be less than the angular size $\sim \pi/2$ of the gate. The MF pulse has to return the pattern in its initial state with the accuracy of the gate size. That is $f^{-1} < \pi/2\Delta m\ \omega_0$ (so the formal solution of Eq. (3) with $\xi = 0$ makes no sense, to be clear in advance). At the same time, the pulse duration may be written in the form $\tau < 0.5\ f^{-1}$. Combining the last inequalities we write:

$$f^{-1} = \frac{\alpha\pi}{2\omega_0},\ \alpha < 1 \text{ and } \tau = \frac{\beta\pi}{4\omega_0},\ \beta < 1. \quad (10)$$

Relation (5) is valid for sinusoidal MFs $H(t) = h\sin(2\pi ft)$, which induces an electric field $E(t) \propto h f\cos(2\pi ft)$. Thermal and galvanic effects are proportional to the time-averaged square of E-field, that is, $\overline{E^2(t)} \propto h^2 f^2/2$. Let the power level W bounds this value that is equivalent to relation (5):

$$h^2 f^2/2 < W \to hf < \sqrt{2W} = k_C. \quad (11)$$

Consider PMF, influencing the same biological system, and write it as the Fourier expansion $H(t) = a_0/2 + \sum_{n=1}^N a_n \cos(2\pi\ nft)$. The frequency spectrum of a PMF must be limited to avoid the infinite power of the induced

electric field. Therefore, pulses are assumed to be approximately rectangular, of duration τ, and the frequency of maximal harmonic N in the expansion to be $\sim\tau^{-1}$, that is, $N\sim 1/\tau\ f$. Find now the value $\overline{E^2(t)}$. After several conversions, taking Fourier coefficients $a_n = 2h\sin(\pi\ n\tau\ f)/\pi n$, we obtain:

$$\overline{E^2(t)} \propto f^2 \sum_{n=1}^{N} a_n^2 n^2 \overline{\sin^2(2\pi\, nft)} = fh^2/\pi^2\tau.$$

Substitution of W from Eq. (11) into the inequality $\overline{E^2(t)} < W$ results in the relation:

$$h\sqrt{f/\tau} < k_C\pi/\sqrt{2} \text{ or } h_{\max} < k_C\pi\sqrt{\tau/2f}. \qquad (12)$$

This replaces the limit (Eq. (5)) in the case of the PMF.

Rule (3) defines ξ values for the series of extremums of P. The difference in $\xi = h\tau$ of the zeroth ($r=0$) and first ($r=1$) extrema equals $2\pi/b$. It means $\Delta h = 2\pi/b\tau$, if we vary the pulse magnitude h and would like to observe two extrema at the h-dependence of the bioeffect. In all cases, there must be $\Delta h < h_{\max}$, we have, combining with Eq. (12), $\Delta h < k_C\pi\sqrt{\tau/2f}$.

Substituting relations for Δh, Eq. (10), and relation $\omega_0 = bH_{\rm dc}$, we obtain:

$$H_{\rm dc} < \left(\alpha\beta^3\right)^{1/4}\sqrt{\frac{\pi^2 k_C}{32\,b}}\ . \qquad (13)$$

The best choice is $\alpha=\beta=1$ (leads to the right part of Eq. (6)), that means a meander-line or square wave PMF.

The last constraint is that the angular shift of the ionic interference pattern, during the reaction time T of the protein, in the absence of PMF, must be larger than the angular size $\sim\pi/2$ of the gate. Otherwise, there is nothing to compensate by a PMF. It results in $\omega_0 T > \pi/2$ or the left part of Eq. (6).

The optimal PMF parameters follow the available value of a static MF. One could find for a given ion $\omega_0 = bH_{\rm dc}$, $f > 2\omega_0/\pi$, $\tau < f^{-1}/2$, and $h < \pi k_C\sqrt{\tau/2f}$. Then, a fine adjustment of the parameters is to be made with rule (3).

References

[1] A.R. Liboff, R.J. Rozek, M.L. Sherman, B.R. McLeod, S.D. Smith, Ca^{2+}-45 cyclotron resonance in human lymphocytes, J. Bioelect. 6 (1987) 13–22.

[2] C. Polk, Biological effects of low-level low-frequency electric and magnetic fields, IEEE Trans. Educ. 34 (1991) 243–249.

[3] H. Berg, L. Zhang, Electrostimulation in cell biology by low-frequency electromagnetic fields, Electro- Magnetobiol. 12 (1993) 147–163.

[4] M. Blank, Electricity and Magnetism in Biology and Medicine, San Francisco Press, San Francisco, 1993.

[5] A. Chiabrera, B. Bianco, J.J. Caufman, A.A. Pilla, in: C.T. Brighton, S.R. Pollack (Eds.), Electromagnetics in Medicine and Biology, San Francisco Press, San Francisco, 1991, pp. 21–31.

[6] V.N. Binhi, Mechanism for magnetosensitive ion binding with a protein, Biofizika 42 (1997) 338–342, in Russian.

[7] V.N. Binhi, Interference of ion quantum states within a protein explains weak magnetic fields effect on biosystems, Electro- Magnetobiol. 16 (1997) 203–214.

[8] V.N. Binhi, Nuclear spins in primary mechanisms of biomagnetic effects, Biophysics 40 (1995) 677–691.

[9] Abstract Book of the 2 World Congress for Electricity and Magnetism in Biology and Medicine, June 8–13, Bologna, Italy. W/L Associates, Frederick MD, 1997, pp. 47, 57, 62, 87, 112, 134, 171, 174, 199, 203, 204, 209, 221, 228, 231, 232, 256, 268, 299, 301, 302, 303, 304, 306, 319, 322.

[10] C.A.L. Basset, The development and application of pulsed electromagnetic fields for ununited fractures and arthrodeses, Orthop. Clin. North Am. 15 (1984) 61–87.

[11] L.D. Landau, E.M. Lifshitz, Quantum Mechanics, Pergamon, Oxford, 1965.

[12] S. Forsen, B. Lindman, Calcium and magnesium NMR in chemistry and biology, Ann. Rep. NMR Spectrosc. 11A (1981) 183–226.

[13] Y.D. Alipov, I.Y. Belyaev, Difference in frequency spectrum of extremely-low-frequency effects on the genom conformal state of AB1157 and EMG2 *E. coli* cells, Bioelectromagnetics 17 (1996) 384–387.

[14] F.S. Prato, J.J.L. Carson, K.P. Ossenkopp, M. Kavaliers, Possible mechanism by which extremely low frequency magnetic fields affect opioid function, FASEB J. 9 (1995) 807–814.

[15] S.M. Ross, Combined DC and ELF magnetic fields can alter cell proliferation, Bioelectromagnetics 11 (1990) 27–36.

[16] R. Goodman, C.A.L. Bassett, A.S. Henderson, Pulsing electromagnetic fields induce cellular transcription, Science 220 (1983) 1283–1285.

[17] R. Goodman, Y. Chizmadzhev, A.S. Henderson, Electromagnetic fields and cells, J. Cell. Biochem. 51 (1993) 436–441.

[18] J. Schimmelpfeng, H. Dertinger, Action of a 50-Hz magnetic field on proliferation of cells in culture, Bioelectromagnetics 18 (1997) 177–183.

[19] J.P. Juutilainen, Effects of low frequency magnetic fields on chick embryos. Dependence on incubation temperature and storage of the eggs, Z. Naturforsch. 41C (1986) 1111–1115.

[20] C.F. Blackman, S.G. Benane, D.E. House, Evidence for direct effect of magnetic fields on neurite outgrowth, FASEB J. 7 (1993) 801–806.

[21] K.A. Jenrow, C.H. Smith, A.R. Liboff, Weak extremely-low-frequency magnetic fields and regeneration in the planarian *Dugesia tigrina*, Bioelectromagnetics 16 (1995) 106–112.

[22] F.S. Prato, M. Kavaliers, A. Thomas, ELF magnetic fields both increase and decrease opioid-induced analgesia in the land snail consistent with the predictions of the parametric resonance model (PRM) for Ca^{2+}, Abst. 18th BEMS Meeting, Victoria, Canada, 1996, pp. 133–134.

[23] E. Berman, L. Chacon, D. House, B.A. Koch, W.E. Koch, J. Leal, S. Løvtrup, E. Mantiply, A.H. Martin, G.I. Martucci, K.H. Mild, J.C. Monahan, M. Sandström, K. Shamsaifar, R. Tell, M.A. Trillo, A. Ubeda, P. Wagner, Development of chicken embryos in a pulsed magnetic field, Bioelectromagnetics 11 (1990) 169–187.

[24] J.M. Farrell, T.L. Litovitz, M. Penafiel, C.J. Montrose, P. Doinov, M. Barber, K.M. Brown, T.A. Litovitz, The effect of pulsed and sinusoidal magnetic fields on the morphology of developing chick embryos, Bioelectromagnetics 18 (1997) 431–438.

[25] F. Bersani, F. Marinelli, A. Ognibene, A. Matteucci, S. Cecchi, S. Santi, S. Squarzoni, N.M. Maraldi, Intramembrane protein distribution in cell cultures is affected by 50-Hz pulsed magnetic fields, Bioelectromagnetics 18 (1997) 463–469.

[26] V. Sollazzo, L. Massari, A. Caruso, M. De Mattei, F. Pezzetti, Effects of low-frequency pulsed electromagnetic fields on human osteoblast-like cells in vitro, Electro- Magnetobiol. 15 (1996) 75–83.

[27] J.L. Phillips, L. McChesney, Effect of 72 Hz pulsed magnetic field exposure on macromolecular synthesis in CCRF-CEM cells, Cancer Biochem. Biophys. 12 (1991) 1–7.

[28] E. Aarholt, E.A. Flinn, C.W. Smith, Magnetic fields affect the lac operon system, Phys. Med. Biol. 27 (1982) 606–610.
[29] O.M. Smith, E.M. Goodman, B. Greenebaum, P. Tipnis, An increase in the negative surface charge of U937 cells exposed to a pulsed magnetic field, Bioelectromagnetics 12 (1991) 197–202.
[30] V.N. Binhi, A Formula for Frequency and Amplitude Windows of Some ELF and Null MF Bioeffects Follows from the Schroedinger Equation, Abstract Book of the 2 World Congress for Electricity and Magnetism in Biology and Medicine, June 8–13, Bologna, Italy. W/L Associates, Frederick MD, 1997, pp. 183–184.